Proceedings World Geothermal Congress 2020+1
Reykjavik, Iceland, April - October 2021

Fractured Geothermal Reservoirs in Iceland: High Temperature Systems From Tectonic Perspective

Maryam Khodayar[1]; Sveinbjörn Björnsson[2]; Egill Árni Guðnason[3], Guðni Axelsson[3], Sigurður Garðar Kristinsson[3], Ragna Karlsdóttir[3], Steinþór Níelsson[3], Magnús Ólafsson[3]

[1]Consultant and Researcher in Geoscience. Kleppsvegur 134, 104 Reykjavik, Iceland

Profnet10@gmail.com; svb@orkugardur.is; Egill.Arni.Gudnason@isor.is; Gudni.Axelsson@isor.is; Sigurdur.G.Kristinsson@isor.is; Ragna.Karlsdottir@isor.is; Steinthor.Nielsson@isor.is; Magnus.Olafsson@isor.is

Keywords: Rift; transform; high temperature; multidisciplinary structural investigations; Iceland

ABSTRACT

High temperature fields in Iceland are within active rifts where heat flow is at maximum. Producing reservoirs are generally between 1 and 3.5 km depth, with 200°C to 350°C temperature. These reservoirs are fracture controlled as faulting and intrusions provide magmatic heat source, permeability and flow paths among other processes. Therefore, in-depth knowledge of tectonic settings is crucial for exploration, production, re-injection, and modelling. Icelandic rift fissure swarms of normal faults, open fractures, dykes, and volcanic centres strike N-S in Northern Rift Zone (NRZ), and NNE to NE in Western Rift Zone and Eastern Rift Zone. The older transform zone of Tjörnes Fracture Zone strikes WNW, has a dextral motion and has three segments, one of which is the Grímsey Oblique Rift. The younger South Iceland Seismic Zone is a general E-W sinistral zone, extending westward to the Reykjanes Peninsula (RP) as an ENE oblique rift, influenced by both rifting and transform faulting there. Within transform segments and oblique rifts, fracturing occurs as strike- and oblique-slip Riedel shears, with frequent earthquakes dominantly on sets of dextral and sinistral conjugate faults. With conspicuous vertical displacements of normal faults and prominent topography of eruptive fissures, geothermal activity has been traditionally attributed to rift-parallel fractures rather than to the Riedel shears. Recent multidisciplinary structural analyses of two high temperature systems, Theistareykir in the NRZ and Reykjanes on RP, revealed the role of transform structures combined with rift from regional to local scales, and from surface to the reservoirs and deeper: (a) The mapped fracture populations can be up to 75% Riedel shears and 25% rift-parallel. (b) Magma injects into rift structures and equally into strike- and oblique-slip faults, some of which are also reactivated during earthquakes. (c) While subsidence occurs mostly on rift structures, the structural compartmentalisation of the reservoirs, alteration, seepage of steam and gases, formation temperature provinces, structural carriers and barriers to flow are dominantly controlled by the Riedel shears. Rotations of resistivity anomalies on the same Riedel shears indicate segmentation of these strike- and oblique-slip faults down to 8 km crustal depth. Selected examples of the above processes from Reykjanes and Theistareykir are presented here.

1. INTRODUCTION

Contrary to oil and gas fields, which are governed by sedimentary, structural and magmatic processes, geothermal systems undergo tectono-magmatic events and are fracture-controlled. Faults and intrusions regulate the permeability, flow, heat source, reservoir compartments and geothermal activity within them. Therefore, comprehensive structural models that incorporate all mechanisms present in geological context(s) should be the basis for interpretation of all data sets, conceptual and reservoir models, in order to reduce the risks of unsuccessful drilling.

The diverging plate boundary has been effective in Iceland since at least 16-15 Ma (Walker, 1960; McDougall et al., 1977), likely 24 Ma (Harðarson et al., 1997), with periodic relocations of spreading centers that resulted in several active and extinct rift and transform segments and widespread associated fracture sets. Geothermal wells are drilled into this highly fractured context where older structures reactivate, younger faults do form, and intrusions inject into the active plate boundaries and into the older crust.

One of the two studied high temperature geothermal systems is Theistareykir at the junction of the active rift and transform segments in North Iceland, and the other is Reykjanes, in the oblique rift of Reykjanes Peninsula (RP) (Fig. 1a). So far, 18 wells drilled in Theistareykir supply a 90 MWe plant, and 37 wells in Reykjanes a 100 MWe operating plant. Wells are generally 2-3 km deep (TVD) with up to 350°C (e.g., Khodayar et al., 2018a; 2018b), except the IDDP-2 in Reykjanes, which reached 535°C at ~ 4.5 km depth (Friðleifsson et al., 2018).

Unravelling the structural configuration of geothermal systems relies on: (a) Instrumental monitoring of crustal deformation and earthquakes for present-day tectonic. (b) Surface mapping of younger fractures of rift and transform zones, providing at best a window back to Holocene. (c) Geological investigations in the older crust. (d) Geophysical and geochemical investigations reflecting past and present geothermal activity at surface and sub-surface. Although instrumental monitoring shows the strong present activity of transform zones (a mechanism that has shaped Iceland for at least 15 Ma), rift-parallel structures are traditionally favored to model permeability and heat source, and used as targets for drilling.

This paper presents selected results of recent multidisciplinary structural investigations, which demonstrate how rifting and transforming combined control the geothermal systems at Theistareykir and Reykjanes.

Note that throughout the paper, the thick colored lines on figures highlight the underlying fractures. They are not arbitrary lines drawn to explain the shape or changes of specific datasets such as resistivity, pressure drawdown, earthquakes, etc.

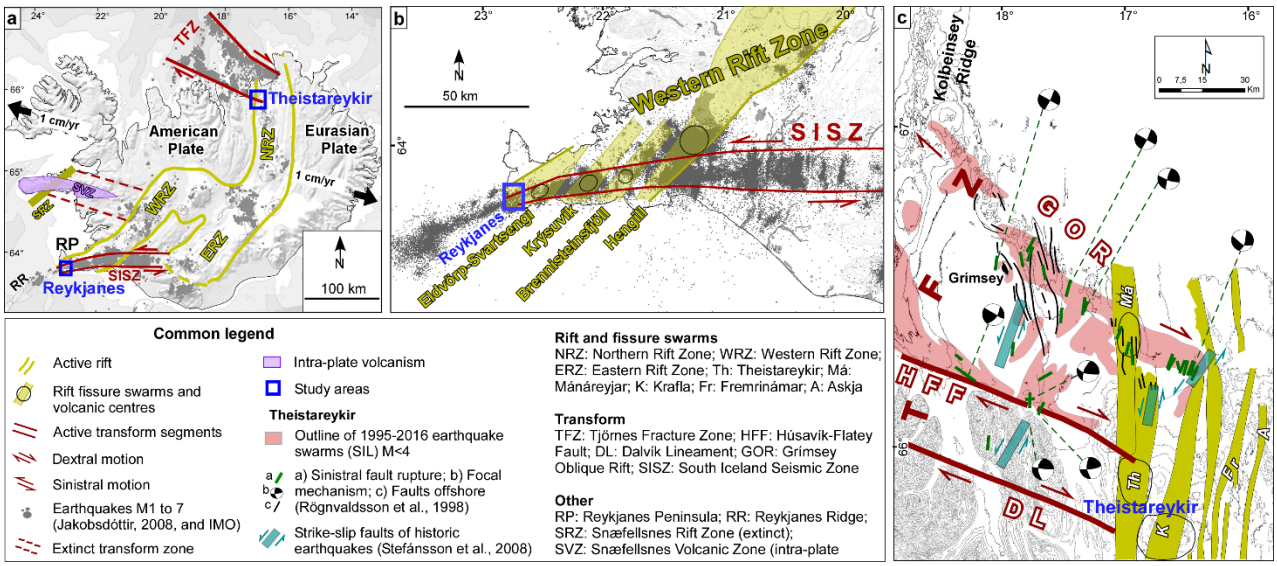

Figure 1: a) Main tectonic elements of Iceland and locations of the study areas. b) Rift fissure swarms and earthquakes at Reykjanes oblique rift. c) Rift fissure swarms, transform zone, and earthquakes at Theistareykir.

2. OVERVIEW OF GEOLOGICAL CONTEXT

The American and Eurasian Plates spread at a rate of 2 cm/yr (Einarsson, 2008) in the direction of N103°-N105° (DeMets et al., 1994) in Iceland. Plate separation occurs along the active segments of Northern Rift Zone (NRZ), Western Rift Zone (WRZ) and the Eastern Rift Zone, the transform zones of Tjörnes Fracture Zone (TFZ) and the South Iceland Seismic Zone (SISZ), and two oblique rifts at RP and Grímsey (GOR) (Figs. 1a to 1c). These plate boundaries are loci of active volcanism, earthquakes and high temperature geothermal activity. Rift fissure swarms consist of parallel normal faults, open fractures, eruptive fissures and caldera (Bodvarsson and Walker, 1964; Sæmundsson, 1978; Arnorsson et al., 2008), striking N-S in NRZ, and NNE on RP. The younger SISZ stretches E-W in South Iceland and ENE on the RP. Without apparent boundary faults, its sinistral motion is accommodated by Riedel shears within this transform segment. The older TFZ strikes WNW and undergoes dextral oblique-slip motion along its three segments of Húsavík-Flatey Fault (HFF), Dalvík Lineament (DL), and GOR, as well as by strike- and oblique-slip motions along Riedel shears within the entire transform zone. The wide strike-range and motions of fractures are explained by severe stress fluctuations (Homberg et al., 2010). Oblique-rifting in RP and GOR occurs through the combination of rift-parallel extensional fractures and the Riedel shears of transform zones.

The Reykjanes geothermal system is at the junction of WRZ and the westward continuation of SISZ (Fig. 1b). The last eruption dates from 13th Century, but the area is mostly covered by postglacial Holocene lavas, with isolate hyaloclastite ridges aged < 0.115 Ma (Björnsson et al., 1972; Franzson, 2004). Being at a young stage of highly oblique rifting, the magma is primitive, and acidic rocks and central volcano are absent from outcrop (Steinthorsson et al., 1986; Armannsson, 2016). Earthquakes are periodic, every 30 years on average, with M_L up to 6 (Einarsson, 2008). The last two earthquake swarms of Reykjanes date from 1972 (Klein et al., 1977), and 2013 (Guðnason and Ágústsson, 2014; Guðnason et al., 2015), with M_L up to 4. Ruptures occur dominantly on conjugate sets of N-S (dextral) and ENE (sinistral) (Einarsson, 2008), and secondarily on WNW and NW faults (Khodayar et al., 2014). Earthquakes are also induced by injection. Left- and right-stepping *en échelon* fracture arrays are surface expression of these deep faults, present in the axes of both the rift fissure swarms on RP (Clifton and Kattenhorn, 2006; Trippanera et al., 2015) and the Reykjanes ridge offshore (Dauteuil and Brun, 1996; Palgan et al., 2017). Surface manifestations indicate that the geothermal reservoir is relatively small (1-2 km^2) in Reykjanes (Khodayar et al., 2014).

Theistareykir geothermal system is in the eastern part of the 9-km wide Theistareykir/Mánáreykjar fissure swarm, and between the HHF and DL (Fig. 1c). The swarm contains postglacial lavas (15000-present), the only Pliocene marine sediments of Iceland in Tjörnes (Eiríksson, 1981; Símonarson and Eiríksson, 2008), and igneous series dating at least 10 Ma (Kristjánsson, 2008). Dykes strike N-S, but they are rare and limited to the eastern and western boundaries of the swarm. The last two eruptions of this swarm occurred onland 2400 yr BP in Stórihver (Sæmundsson et al., 2012), and offshore in 1868 in Mánáreyjar (Thoroddsen, 1925). Despite local acidic rocks in outcrops and wells, this fissure swarm lacks a collapse caldera. Regional earthquakes related to transform faulting, with M < 7, occur on NNE to ENE sinistral, and WNW to NW dextral Riedel shears (Rögnvaldsson et al., 1998), but large earthquakes are rare in the geothermal system. Surface geothermal manifestations indicate that the reservoir is at least 7 km^2, and likely larger at depth.

Until recently, geothermal activity has been mainly attributed to rift structures striking N-S in Theistareykir and NNE in Reykjanes. Examples below show the role and frequency of rift and transform fracture sets in the surface and subsurface geothermal activity of these two areas.

3. OBSERVATIONS

3.1. The structural patterns

Results below are selected from extensive multidisciplinary structural investigations of Theistareykir and Reykjanes, carried out respectively for Landsvirkjun and HS Orka as a part of geothermal exploration for drilling and conceptual modelling. The

methodology includes first a thorough interpretation of faults, dykes, open fractures, and source faults of earthquakes on several aerial images and DEM, outcrop checking, interpretation of the tectonic deformation, and relative fracture evolution. Results were used to interpret these multidisciplinary data sets: surface geothermal manifestations (gases, alteration, fumaroles), resistivity anomalies, earthquakes, well stratigraphy and feeders, formation temperature, pressure drawdown, etc., to better understand the structural configuration of the reservoirs. The outcome was the ground for proposing well sites and structural drilling targets.

Six sets of fractures emerge in the structural architectures of Reykjanes (Fig. 2a) and Theistareykir (Fig. 2b). At Reykjanes, these sets strike N-S (0˚-N27˚E), NNE/NE (N28˚-N40˚E), ENE (N41˚-N75˚E), E-W (on average N90˚E), WNW (N115˚-N130˚E), and NW/NNW (N140˚-N155˚E and N165˚E) in Holocene lavas. Although the NE and NW sets appear dominant in the total fracture population, locally, the ENE and N-S fractures are also prominent in the reservoir area. The E-W set is the least frequent. Fractures have strong or subtle traces, and are segmented with lengths of a few meters up to 2 km. Fractures are dominantly faults as dykes are rare. All sets have dip-slip (<0.5 m to 15 m), with the highest slips on ENE, N-S and NE faults. Right- and left-stepping *en échelon* arrays indicate sinistral motion on ENE faults and dextral motion on N-S faults (Figs. 3a and 3b). However, WNW and NW fractures also display dextral motion. Secondary fractures, similar to those present in the reservoir (Figs. 3c and 3d), strike along the six sets, while surface ruptures of earthquakes (open fractures, sink-holes and push-ups) are dominantly N-S and ENE but also WNW (Fig. 3e) similar to the organization of surface geothermal manifestations (Figs. 3f and 3g). Given the spreading at N103°E in Reykjanes, NNE fractures would be rift-parallel extensional fractures, while the other sets would act as the oblique-slip Riedel shears of the transform zone (Fig. 2a). The origin of the WNW and NW sets is unknown. They could be two sets among the Riedel shears, horsetail splay of each other, transfer zones similar to those offshore RR (Hoskuldsson et al., 2004) or on land (Franzson, 2004), or a part of an older transform zone onshore (Khodayar et al., 2014). Aspects related to dykes and push-ups are further discussed in later chapters.

The fracture sets at Theistareykir strike N-S (0˚-N20˚E), NNE (N21˚-N50˚E), ENE (N51˚-N80˚E), E-W (N81°-N100°E), WNW (N101˚-N130˚E), and NW/NNW (N131˚-N170˚E), in the crust spanning at least 10 Ma to 2400 yrs BP (Fig. 2b). The N-S, ENE, WNW, and NW sets are the most frequent and the E-W the least. Except for two limited N-S dykes at the boundaries of the Theistareykir fissure swarm, the structures are faults, joints and open fractures. Fractures are at various stages of evolution, i.e., younger in postglacial lavas and older in the bedrock. They are segmented, ranging from ~5 m to 5 km in length. Extension is associated with all sets, expressed either as dip-slips of 0.5-5 m in the 2400 yr lava, 5-20 m in post-glacial series, and 200 m in bedrock, or as apertures up to 3 m along open fractures. Older fractures have sharper topographic signature, while younger normal and strike-slip faults, tension gashes and joints have subtle traces. The overall structural pattern is a combination of N-S rift-parallel extensional fractures, and the Riedel shears of transform zone striking NNE to ENE with sinistral motion, and dextral motion on WNW to NW sets based on their *en échelon* arrangements (Figs. 3h and 3i). Surface alteration is clearly aligned along these Riedel shears (Fig. 3j). Evidence was inconclusive for the sense of strike-slip along the E-W set. The identified strikes and motions are identical to those in regional and local earthquakes (Fig. 1c), and compatible with regional stress fields leading to normal and strike-slip fault regimes (Homberg et al., 2010).

Some structural features are common to both areas. (a) The magnitude of strike-slips could not be determined along any set due to lack of marker horizons. (b) Statistical analysis of fractures vs. relative rock age in Theistareykir shows that fractures form under the influence of transform regime, and rift structures develop with time, without becoming dominant, however (Khodayar et al., 2018b). Reykjanes could be subject to the same fracture formation and evolution. (c) Fracture segments coalesce during their evolution, accumulate slips and evolve into major faults. As strike-slips, especially the youngest, are subtle and without dip-slips, they are overlooked and underestimated in structural patterns. (d) Several weak zones exist in each area (Figs. 4a and 4b). They are zones of higher fracture density and/or wider *en échelon* arrays when above deeper faults, or have prominent pronounced trace and/or displacement when individual fault has broken the surface (Khodayar and Björnsson, 2018). These zones appear along any set, are widely distributed in Theistareykir (Fig. 4b), but are organized at or within two ENE zones in Reykjanes, i.e., the Northern and Southern Riedel Shear Zones. Fracture density is higher in the latter zone where the rift-parallel structure of Rauðhólar presents an obvious clockwise rotation (Fig. 4a).

3.2. Intrusion into shear fractures

Eruptions and dyke injections are generally explained in terms of pure extension. In Iceland, they are traditionally seen as being parallel to normal faults of rift within fissure swarms. At Reykjanes, the Rauðhólar-Sýrfell and Litla-Vatnsfell ridges strike ~NE and were formed in sub-glacial eruptions through rift-parallel structures. However, the few surface dykes in Rauðhólar strike dominantly ENE and N-S similar to faults of earthquakes, and secondarily NE (Fig. 5a). Farther east, the eruptive craters of Klofningar in Eldvörp display a typical right-stepping *en échelon* arrangement in the continuation of a major ENE sinistral oblique-slip fault relevant to geothermal activity (Khodayar et al., 2018a). As further discussed in chapter 4.3 below, fault plane solutions of 1972 earthquakes (Klein et al., 1977) also show oblique-slip motion on this structure (Fig. 5b). At Theistareykir, N-S eruptive fissures are absent from outcrop and the eruption of 2400 yr BP occurred perpendicular to this fissure swarm on the WNW Stórihver Fault that has dextral motion and is parallel to the HFF (Khodayar, 2018). The main segment of the Stórihver Fault and its horsetail splay (Figs. 5c to 5e) enter the geothermal reservoir to the east with a dominant role there (Khodayar et al., 2018b). Dyke injection into shear faults was first described in West Iceland (Khodayar and Einarsson, 2002), and recently reported during the 2014 fissure eruption of Holuhraun (Sigmundsson et al., 2015). These are few examples of magma injection into shear fractures in presence of rifting.

4. STRUCTURAL INTERPRETATIONS OF MULTIDISCIPLINARY DATA

4.1. Surface manifestations, alteration and gases

At Reykjanes (Figs 6a to 6c), surface alteration ranges from mild to severe with 11° to < 100° C temperature. The mildest is unaltered rock with occasional steam, and the severe form is the rock entirely altered to clay. The same temperature ranges apply to mild steam, fumaroles, solfataras, boiling mud pools and vigorous steam vents. The structures beyond which surface manifestations are absent are the NE-striking sinistral oblique-slip Litla-Vatnsfell Fault to the west, and other ENE sinistral oblique-slip segments and surface ruptures to the east, which are the last permeable structures from which steam can escape from the reservoir towards surface. In the center of the reservoir, the structural compartmentalization between high and low alteration, and the alignments of fumaroles to steam

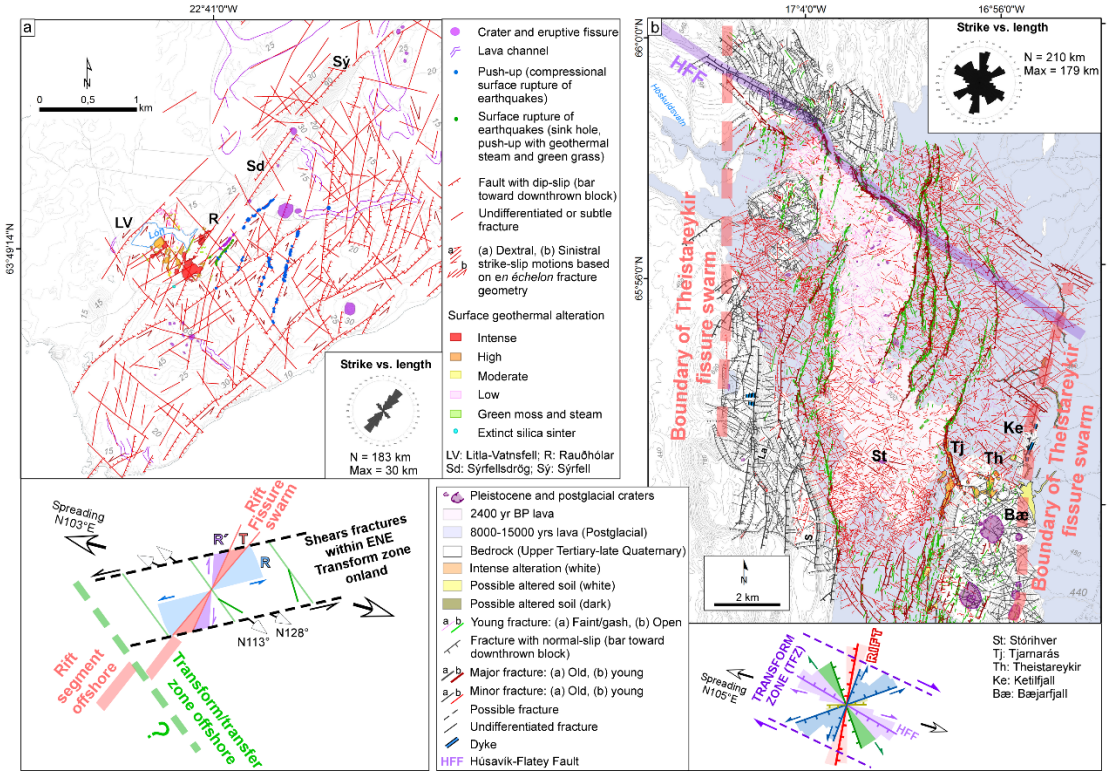

Figure 2: a) Structural pattern of Reykjanes geothermal system at the oblique rift on RP, fracture frequency and motions (modified from Khodayar et al., 2018a). b) Structural pattern of rift and transform zone at Theistareykir, fracture frequency and motions (modified from Khodayar et al., 2018b).

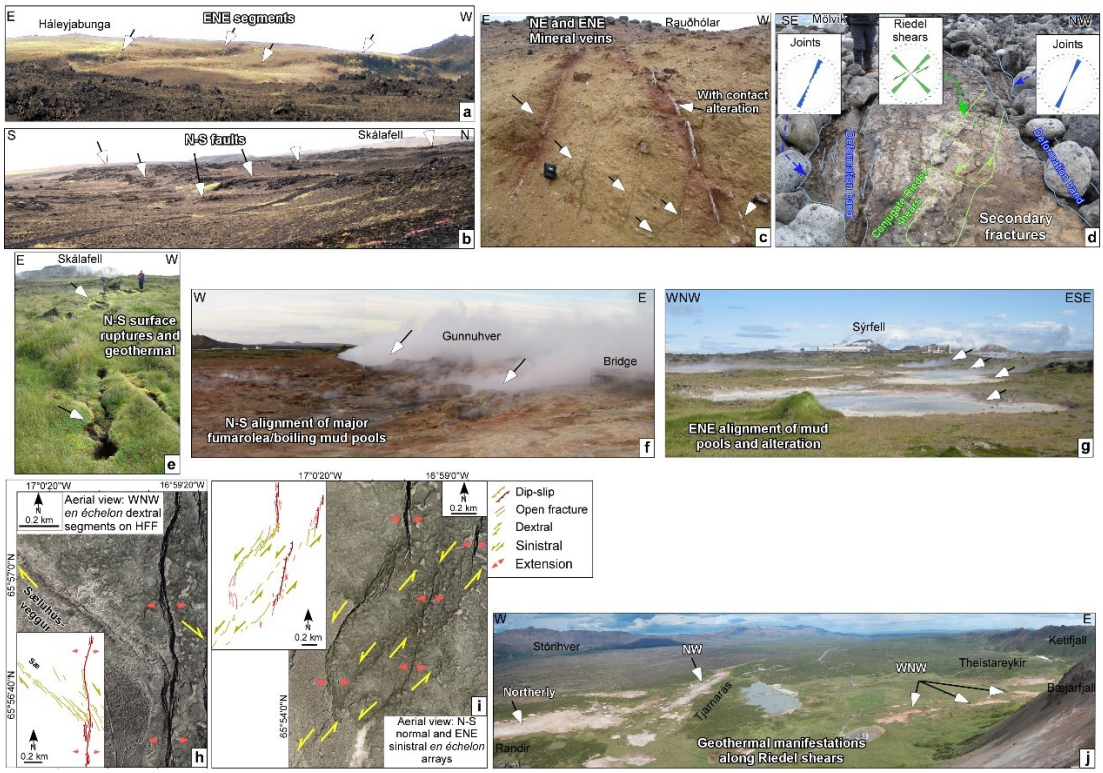

Figure 3. Examples of fracture types and surface geothermal activity. a) Right-stepping *en échelon* arrays along the sinistral oblique-slip reservoir boundary fault at Reykjanes. b) Dip-slip on parallel N-S dextral oblique-slip faults at Reykjanes. c) Mineral veins, d) secondary Riedel shears and breccia, e) dextral strike-slip surface ruptures of earthquakes with geothermal activity, f) biggest fumaroles aligned in NNE left-stepping arrays typical of dextral motion, g) major alteration and fumaroles in right-stepping arrays typical of sinistral motion at Reykjanes (modified from Khodayar et al, 2018a). h) Young WNW left-stepping *en échelon* segments reflecting dextral motion on Húsavík-Flatey Fault, i) Right-stepping *en échelon* NNE to ENE arrays indicative of sinistral motion, j) surface alteration aligned NW, northerly and WNW at Theistareykir (modified from Khodayar et al., 2018b).

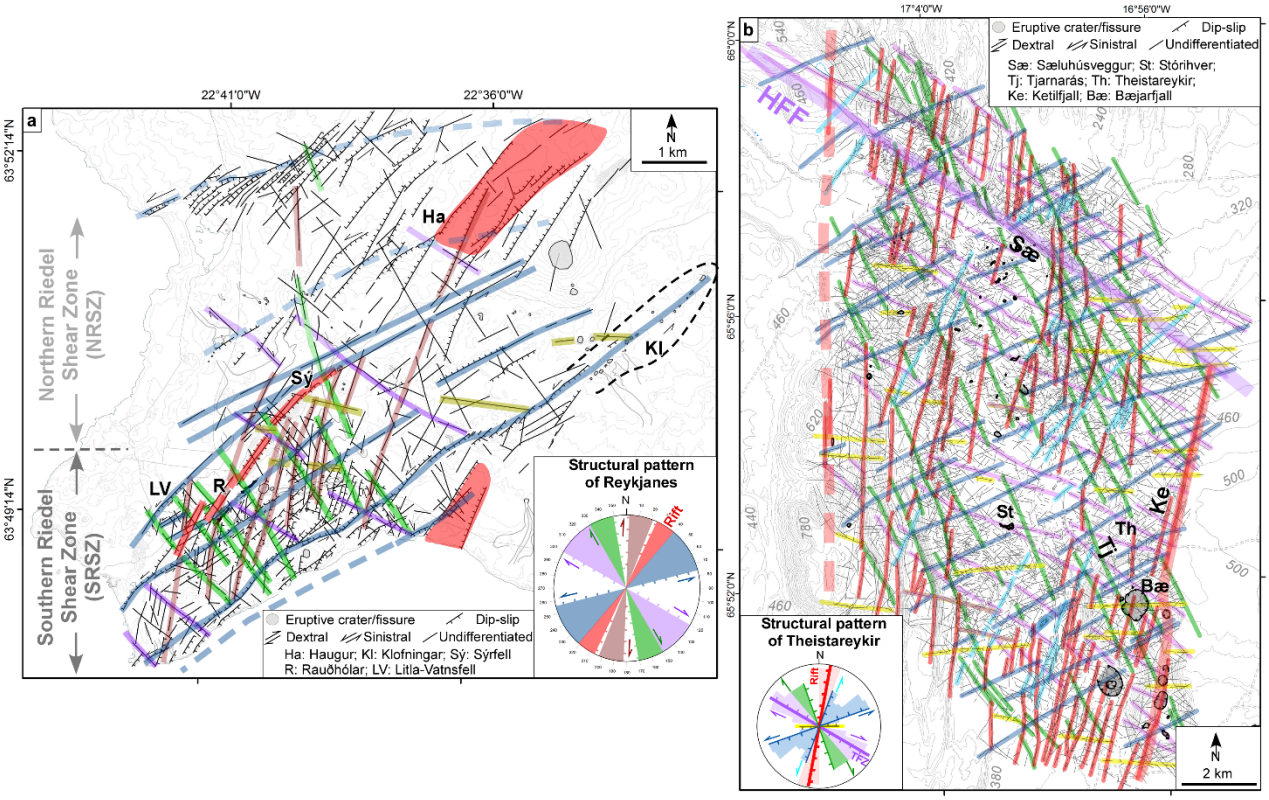

Figure 4: a) Highlights of the structural weak zones of Reykjanes within the ENE Northern and Southern Riedel shear zones, and recall of their motions. Note the rotation of Litla-Vatnsfell Fault and Rauðhólar rift segments by the ENE sinistral boundary between the two shear zones (modified from Khodayar et al., 2018a). b) Highlights of the structural weak zones at Theistareykir and recall of their motions (modified from Khodayar et al., 2018b).

vents, all occur on these structures: a major N-S dextral fault zone crossing the middle of the lagoon (Lón), series of parallel ENE sinistral oblique-slip and WNW/NW oblique-slip dextral faults. The NNE rift segments parallel to Rauðhólar appear to play a role in surface temperature distribution. The same Riedel shears control the CO_2 flux (Khodayar et al., 2018a), and the alteration in wells (Khodayar et al., 2014).

Similar configurations govern Theistareykir (Figs. 6d and 6e). Surface alteration is contained in a block bounded by NE/ENE sinistral oblique-slip faults, the NW and WNW Tjarnarás and Stórihver dextral oblique-slip faults, the N-S eastern boundary fault of Theistareykir fissure swarm at Ketilfjall, along with a short N-S fault at Randir. Within this block, other faults parallel of these sets regulate the distribution of surface alteration, but the role of the N-S faults is minimal. The distribution of fumaroles, solfataras, mud pools and steam vents is also controlled by the same fractures of the four Riedel shear sets along with a few short N-S segments (Khodayar et al., 2018b). Gas flux (Gíslason et al., 1984), and feeders in wells also align dominantly on the same Riedel shears, and to a lesser degree on the same N-S short fault segments (Khodayar et al., 2014).

4.2. Tracer flow paths and carrier/barrier structures

Only examples from Reykjanes are presented here. To assess the flow channels and fracture permeability, tracers were injected in two production wells RN-20b (August 2013), and RN-33 (January 2014) and their arrivals monitored in other wells. Three datasets were used for their structural interpretation: distribution, amount and arrival time of tracers; pressure drawdown at 1600 m depth; and the comprehensive structural map of rift and transform fracture sets in Reykjanes (Figs. 7a to 7e). Tracers may have entered the formation at 1144 m (TVD) in RN-20b and at 2015 m (TVD) in RN-33. They arrived in other wells after 77 to 133 days from RN-20b, and 24 to 333 days from RN-33. The tracer from RN-33 flowed from east-northwest towards west-southwest on paths 1 to 5. It likely travelled successively along these carrier structures: the NNE segments of Rauðhólar/Sýrfell, a NW-striking dextral oblique-slip fault, and an ENE sinistral oblique-slip fault that includes surface ruptures of earthquakes (Khodayar et al., 2018a). The tracer, however, did not show up in wells to the west of the reservoir as the N-S fault segments in the middle of the lagoon act as barrier. The tracer from RN-20b flowed west, and travelled likely first along a WNW dextral strike-slip fault and the same ENE fault that acted as barrier in the flow from RN-33. It showed up with a low concentration along paths 2, 3 to 7 and 9 in wells that are on the hanging wall blocks the ENE, the NNE and the N-S barrier structures. Figures 7b and 7d show the dip directions of these faults and how the same fault can act as carrier or barrier depending on the provenance of tracers. It is pointed that these carriers and barriers are the same faults as controlling the surface manifestations, as well as the CO_2 flux, and gas distribution. Regarding the pressure drawdown, its center falls on the NNE segments of Rauðhólar, but its overall elongation and internal changes coincide with ENE, N-S and WNW Riedel shears (Fig. 7e).

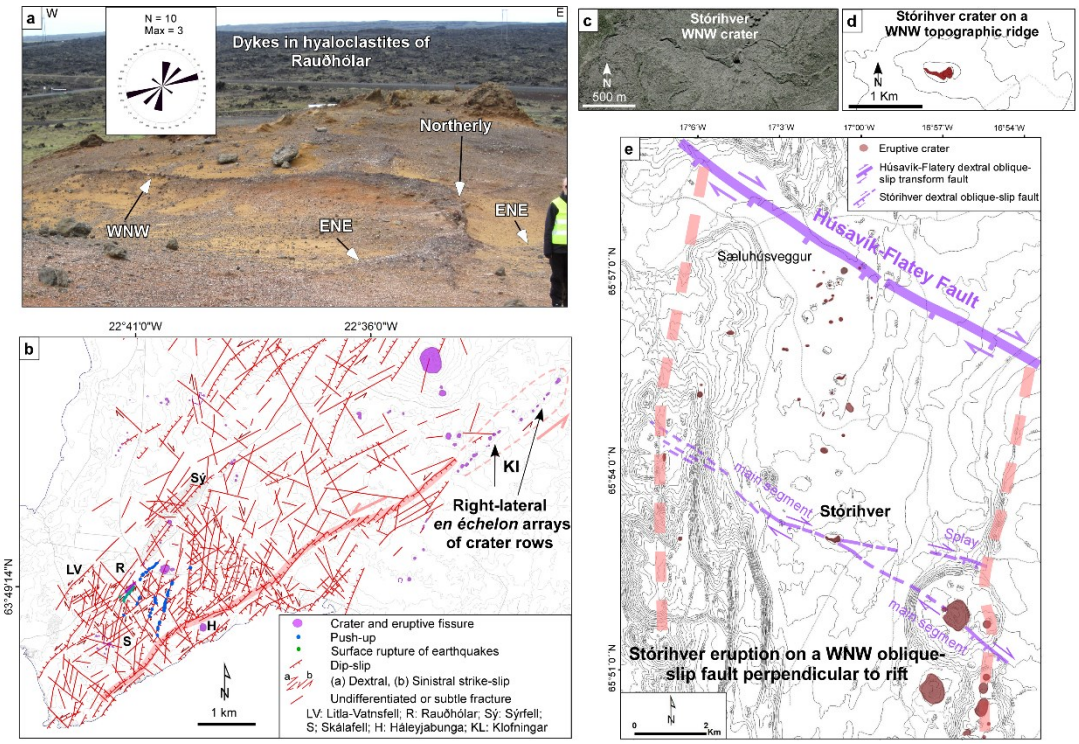

Figure 5: Examples of magma injection into shear fractures. a) ENE, N-S, NE and WNW dyke segments in the hyaloclastites of Rauðhólar above Reykjanes geothermal reservoir. b) Right-stepping *en échelon* arrays of eruptive craters at Klofningar in continuation of the major ENE sinistral oblique-slip fault bounding the Reykjanes reservoir (modified from Khodayar et al., 2018a). c) to e) Morphostructural features of Stórihver crater, the eruptive WNW deep dextral oblique-slip fault and its splay segment that extend into Theistareykir geothermal reservoir (modified from Khodayar, 2018).

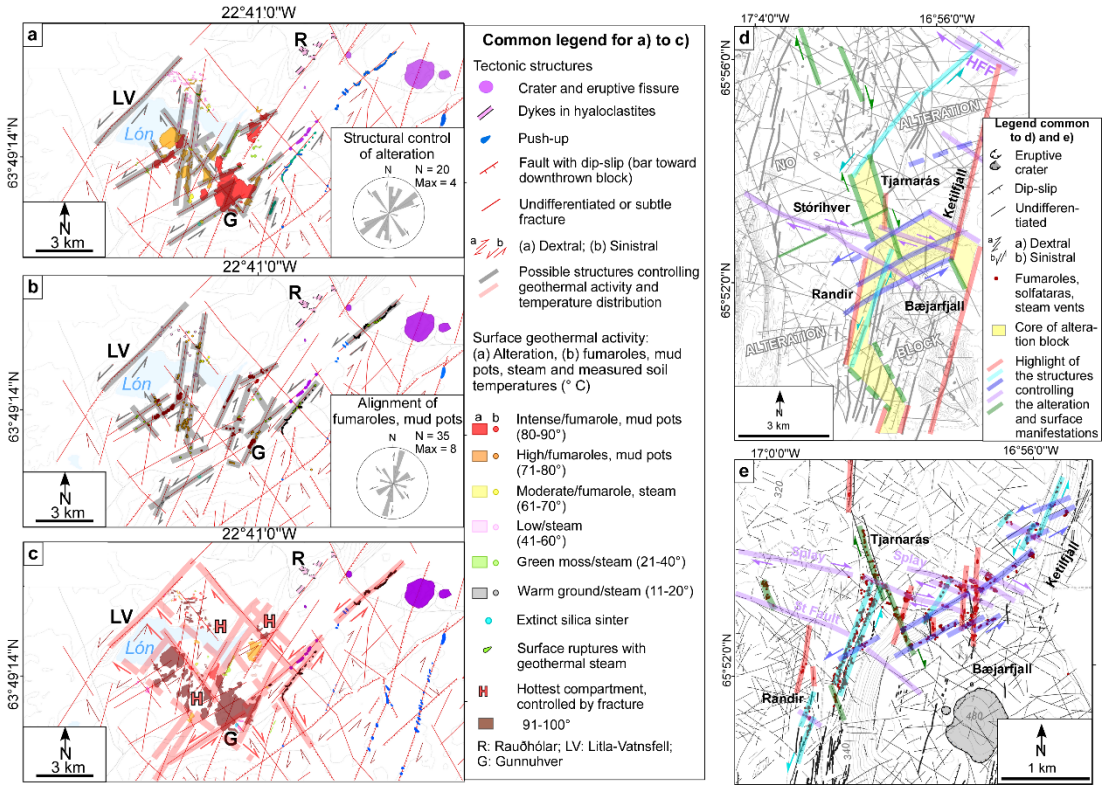

Figure 6: Tectonic control of surface geothermal manifestations at Reykjanes and Theistareykir. a) Surface alteration, b) alignment of fumaroles, mud pools and steam vents, c) soil temperature at Reykjanes and the fracture sets controlling them (modified from Khodayar et al., 2018a). Highlights of rift and transform fracture controlling: d) the boundaries of the alteration block, and e) the alignment of surface manifestations at Theistareykir (modified from Khodayar et al., 2018b). Fumaroles and solfataras were mapped by Kristinsson et al., 2015.

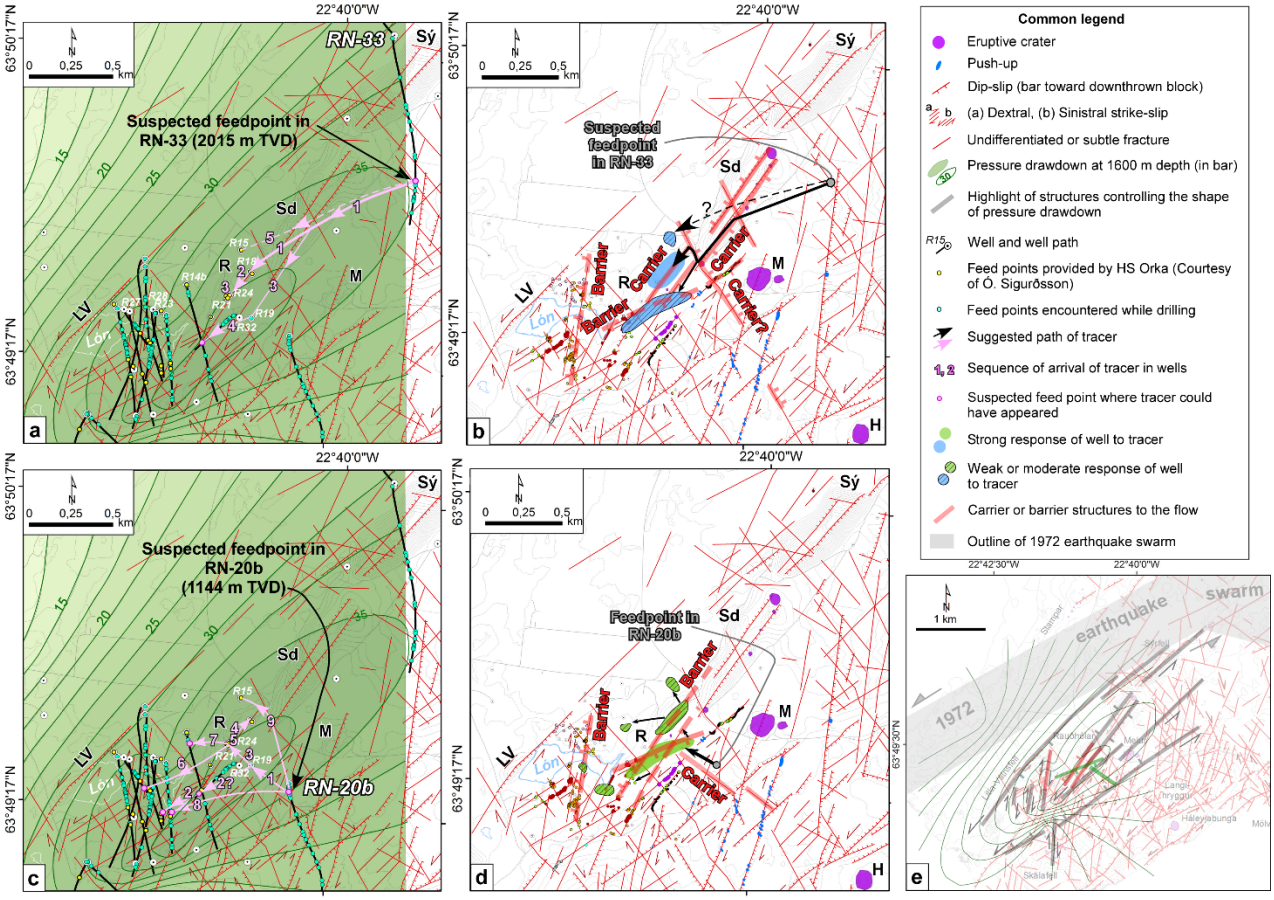

Figure 7: Pressure drawdown (courtesy of Ó. Sigurðsson, HS Orka, 2014), carrier and barrier structures within the reservoir based on arrival time of tracers. a) and b) From RN-33, c) and d) from RN-20b (modified from Khodayar et al., 2014; 2018a). e) Structural control of the pressure drawdown isolines.

4.3. Earthquakes and structural compartments

Seismo-tectonic configuration at Reykjanes and Theistareykir are summarised here (Figs. 8a to 8e). The main earthquake swarms on RP occurred in 1972 onland (Klein et al., 1977), and in 2013 offshore (Guðnason and Ágústsson, 2014). They had 2-6 km crustal depth, and up to ML 4 in magnitude. Each swarm falls within a narrow ENE zone, coinciding with the ENE sinistral boundaries of the Northern (NRSZ) and Southern Riedel Shear zones (SRSZ) (Figs. 4a, 8a and 8b). Their fault plane solutions (FPS) show pure sinistral motion on ENE, dextral on N-S, normal-slip on NE, ENE, WNW and NW fault planes, and a few oblique-slip motions on these sets, matching the structural map (Figs. 8a and 8b). The distribution of FPS compared to the structural weak zones is critical. Those of 1972 fall only in area (A) of the NRSZ, but also on the ENE eruptive fissure of Klofningar, which is on the boundary of the SRSZ (Fig. 8a). The FPS of 2013-2015 earthquakes are more complex: A blend of dip-slip and strike-slip FPS in areas (A1) of the SRSZ to the west of Rauðhólar, all dip-slip FPS in area (A2) of the NRSZ, and all strike-slip FPS inside area (B) of the SRSZ (Fig. 8b). Seismic lineations of both swarms also align dominantly N-S, ENE, and WNW, and to a lesser degree E-W.

The major structural compartments deduced from seismo-tectonic are (Khodayar et al., 2018a): (a) A cluster within the 1972 swarm aligns NNE and intrudes from the ENE zone into the wide rift-parallel Haugur Graben (Figs. 8a to 8c). It indicates that during transform episodes, earthquakes "leak" into extensional rift structures and reactivate them. (b) An equivalent to this graben does not exist within the SRSZ. There, the rift-parallel structures are segments of Rauðhólar, which, along with the Litla-Vatnsfell structure, rotate clockwise from NNE to ENE at the approach of the 1972 swarm (Fig. 8c). Compression is expected to the east of this rotated structure where in fact compressive push-ups and the reverse-slip FPS are all located. (c) In the middle of the 1972 swarm, one earthquake cluster aligns WNW on the traces of weak zones, and extends from the NRSZ southeastward to the coast. This particular WNW structure bounds a highly fractured Block (1) containing the reservoir, from a lesser deformed Block (2). The WNW structure has also been found in newer analysis of earthquakes and resistivity (Karlsdóttir et al., 2018). Finally, the 2013-2015 earthquakes reveal an aseismic body under the geothermal field, above the brittle-ductile boundary of 6 km (Guðnason et al., 2015). This body is attributed to episodic activity, pore pressure reduction due to production, or to a hot body (> 600˚C ± 100˚C) at depth. It falls within the SRSZ and the reservoir, bounded by ENE and WNW fractures (Fig. 8d).

Fewer earthquakes are recorded at Theistareykir from 1993 to 2011 (Hjaltadóttir and Vogfjörð, 2011) and in 2014-2015 (Ágústsson and Guðnason, 2016). The 1993-2011 earthquakes span 3 to 7 km depth, with magnitudes -0.6 ≤ ML ≤ 3.2. (Fig. 8e). They fall into clusters 1 to 4, have complex and alternative FPS, but fit best with these structures of the reservoir: the NW Tjarnarás and WNW Stórihver dextral oblique-slip faults (c. 1 and 2), the NNE sinistral oblique-slip Randir Fault (c. 3), and a WNW dextral oblique fault north of Bæjarfjall (c. 4). The 2014-2015 earthquakes are mostly in Bæjarfjall, 2-4 km deep (although some reach 6 km), with ML 1 to 1.9. Their seismic lineations fit two main weak zones: the ENE sinistral oblique-slip segments at the southern boundary of the alteration block, and the tightly parallel WNW dextral oblique-slip segments including the Stórihver Fault. FPS show the dextral

motion of this latter fault. The main structural compartments and their internal fracturing are dominantly the Riedel shears of the transform zone (WNW, ENE, NW and E-W) and secondarily rift-parallel (N-S). Both control all aspects of geothermal activity. The earthquakes only reflect the activity of few of the critical structures.

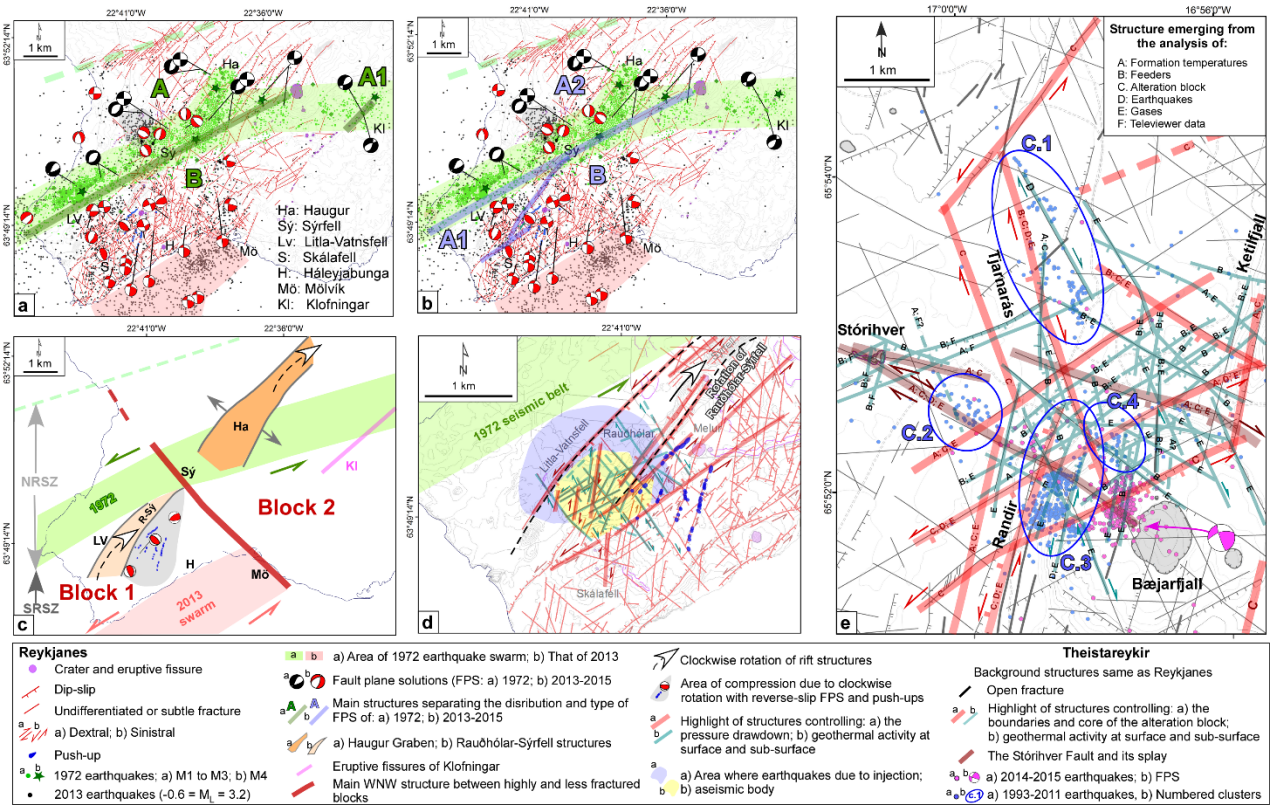

Figure 8: Seismo-tectonic and structural compartmentalisation at Reykjanes (modified from Khodayar et al., 2018a) and Theistareykir (modified from Khodayar et al., 2018b). a) and b) The 1972 and 2013 earthquake swarms and the FPS of 1972 (Klein et al., 1977) and 2013-2015 earthquakes (Ágústsson and Guðnason, 2014) compared to major structural weak zones at Reykjanes. c) Boundaries of earthquake swarms and the ENE Riedel shear zones, the reactivated Haugur Graben, the clockwise rotation of rift-parallel structures, and a major WNW structure between the highly (Block 1) and less fractured (Block 2) compartments at Reykjanes. Reverse-slip FPS of 2013-2015 earthquakes and the push-ups are in the area of compression due to rotation. d) Structural control of Reykjanes geothermal reservoir and the aseismic body. e) Major and minor structural compartments at Theistareykir and distribution of earthquakes.

4.4. Resistivity anomalies

Example of resistivity anomalies is selected from Theistareykir where a 3D inversion of MT data reveals the geothermally altered bodies (Karlsdóttir et al., 2012), with a spectacular tectonic control (Khodayar et al., 2018b). The cap rock is shallow (zeolite/smectite alteration zone), on top of a high resistivity core (chlorite/epidote alteration zone), and a deeper low resistivity body indicative of heat source and upflow zones into the geothermal reservoir. Resistivity anomalies display strong left- and right-stepping *en échelon* arrangements, typical of dextral and sinistral structures, and the width of individual anomalies can be from <1 km to ≥ 4 km. Their correlation with the mapped structures shows that they are bounded by series of fractures rather than resulting from fluid flow along a single permeable fracture in the middle of each anomaly. Figures 9a to 9f show that these anomalies rotate with depth. From surface down to 4000 m b.s.l. (0 to 1000 m not shown here due to space), there is a gradual and clockwise rotation of the anomalies and their bounding fractures, i.e., WNW and NW dextral oblique-slip, and NNE to ENE sinistral oblique-slip Riedel shears (Figs. 9a to 9d). The ENE set, however, appears as a clear and dominant set mostly from 2500 to 4000 m b.s.l. Two WNW segments, including the HFF, form a deformation zone to the west. In this WNW zone, shorter N-S resistivity anomalies are bounded by rift-parallel structures, much like extensional pull-aparts associated with major strike-slip faults. There is an anti-clockwise rotation of these structures at 5000 m and 6000 m b.s.l. In this depth range, the E-W set becomes more established and controls a major anomaly to the north of the reservoir along with the NW, WNW and the ENE sets (Fig. 9e). A clockwise rotation of the anomalies and fractures appears again at 8000 m b.s.l., where the E-W and N-S sets are dominant. The N-S set is confined to the west of the study area, and a few NW structures still bound the deepest resistivity anomalies to the east (Fig. 9f). It is noteworthy that the resistivity anomaly below the geothermal area appears clearly only from 2000 m b.s.l. down to 8000 m b.s.l. and is controlled by NW, ENE and E-W fractures. These rotations reflect the dominance of the Riedel shears of the transform zone in the alteration process down to 8 km crustal depth.

5. CONCLUSIONS

Rifting has been the preferred model to interpret the geothermal processes of Reykjanes and Theistareykir high temperature geothermal systems, respectively at a highly oblique rift and at the intersection of rift and transform zones. In fact, subsidence and a part of intrusion and permeability occur on rift-parallel structures. However, thorough multidisciplinary structural investigations show that strike- and oblique-slip fractures resulting from transform activity control the reservoir boundaries and the geothermal activity within them (Figs. 10a and 10b). These shear fractures regulate the surface geothermal manifestations, gas distribution, surface and sub-surface alteration, and permeability. Depending on their dip directions, they also act as dominant carrier or barrier structures to the flow within the reservoirs. Magma equally injects into these Riedel shears, indicating that oblique rifts and transform zones can be magmatically leaky. This common process is often underestimated despite its critical implication for heat source, brecciation in damage zones and fracture permeability. During seismo-tectonic activities related to transform mechanism, such Riedel shears rupture within at and within the reservoirs. Their ruptures also lead to regional block compartmentalizations, dividing the crust into highly and less fractured blocks, and even separation of geothermal systems. During these processes, transform-related earthquakes can also reactivate rift structures. Rotations of resistivity anomalies and rift structures also occur on such Riedel shears that could create local compression within blocks and reduce permeability. Such tectonic is not local, but has a regional character onshore and offshore Iceland (Khodayar and Björnsson, 2018).

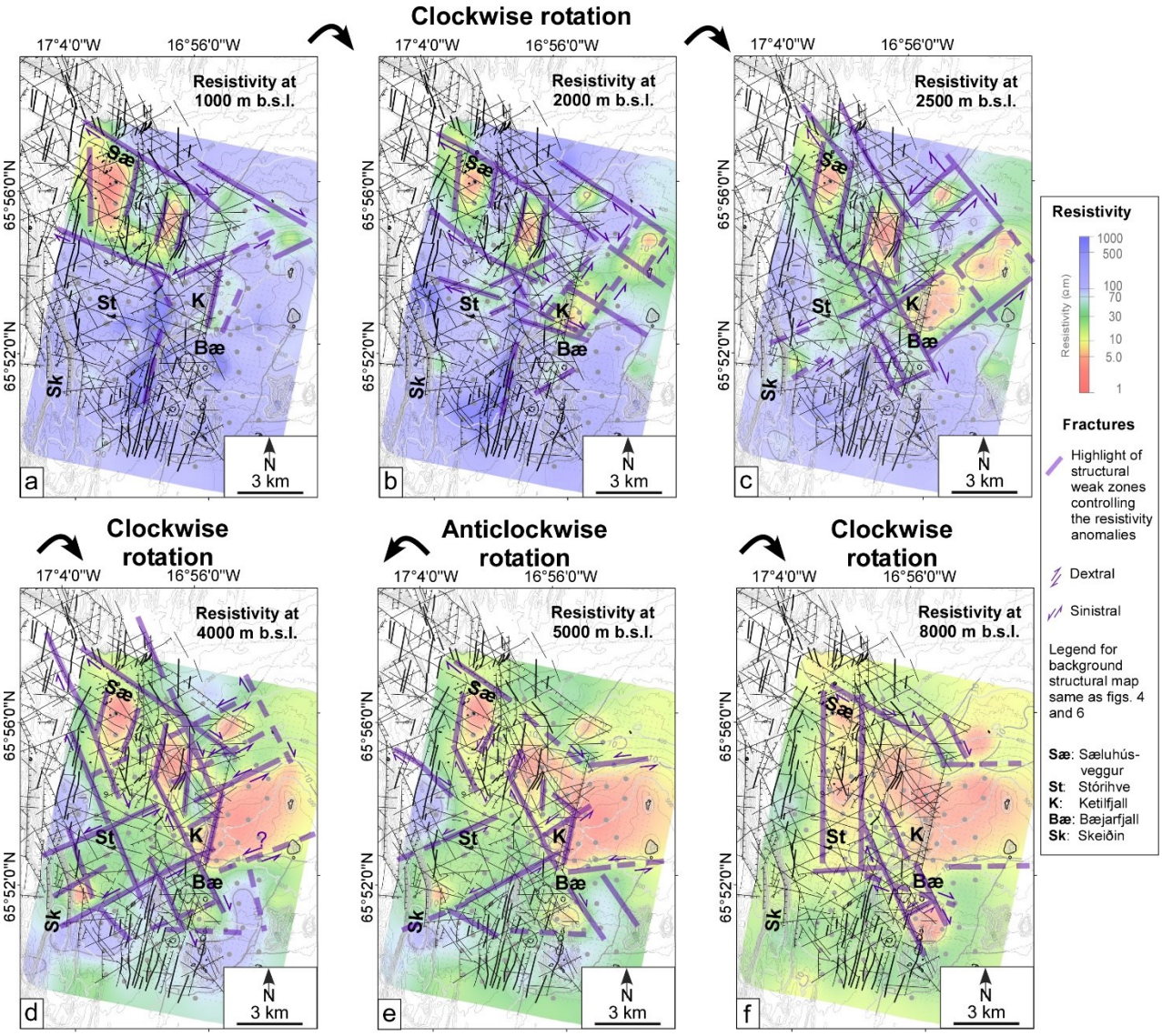

Figure 9: Resistivity anomalies (Karlsdóttir et al., 2012) and their structural interpretation (Khodayar et al., 2018b) at Theistareykir. a) to f) Control of resistivity anomalies by WNW, NW, ENE, and E-W Riedel shears of transform zone and N-S rift-parallel structures, showing a gradual clockwise rotation down to 4000 m b.s.l., an anticlockwise rotation at 5000 (to 6000) m b.s.l., and a clockwise rotation again at 8000 m b.s.l.

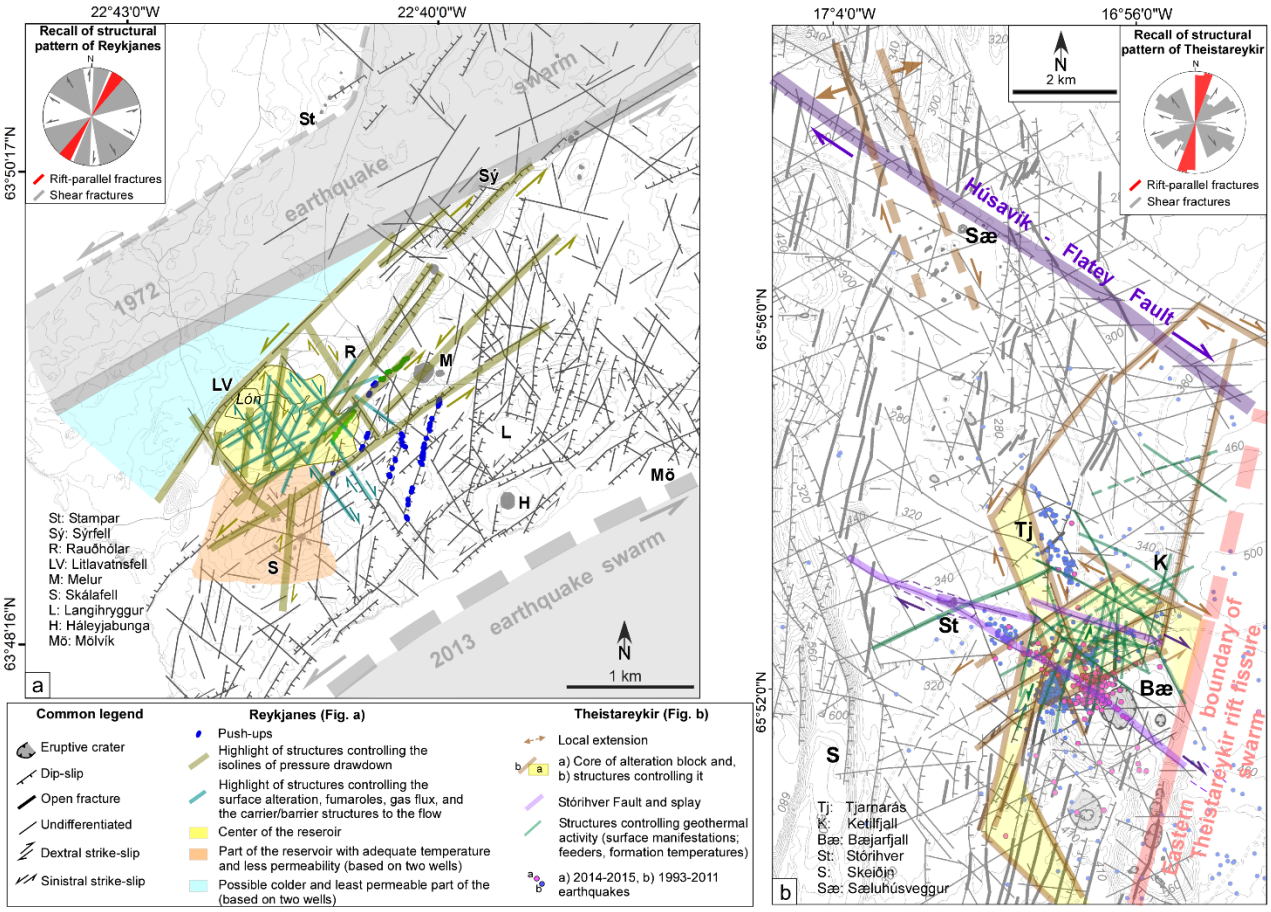

Figure 10: Main results of the multidisciplinary structural investigations at Reykjanes (modified from Khodayar et al., 2014; 2018a) and Theistareykir (modified from Khodayar et al., 2018b). a) The ENE, N-S, WNW shear fractures and the rotated NNE rift structures controlling the reservoir boundaries, pressure drawdown, alteration, surface geothermal activity, and the flow within the Reykjanes geothermal reservoir. b) The main structural compartments at and within Theistareykir reservoir, controlled dominantly by the WNW, ENE, NW and NNE Riedel shears of the transform zone and N-S rift-parallel fractures, as well as earthquakes on these Riedel shears.

ACKNOWLEDGMENTS

The authors wish to thank HS Orka and Landsvirkjun for commissioning the data collection and interpretations, and for their permission to publish the results. The initial data analyses and interpretations were carried out while Maryam Khodayar was a staff of Iceland GeoSurvey (ÍSOR).

REFERENCES

Armannsson, H.: The Fluid Geochemistry of Icelandic High Temperature Geothermal Areas. *Applied Geochemistry*, **66**, (2016), 16-64. https://doi.org/10.1016/j.apgeochem.2015.10.008

Arnorsson, S., Axelsson, G. and Sæmundsson, K.: Geothermal Systems in Iceland. *Jökull*, **51**, (2008), 269-302.

Ágústsson, K. and Guðnason, E.Á.: Focal Mechanism of Selected Earthquakes at Þeistareykir (in Icelandic). Iceland GeoSurvey Short Report, ÍSOR-16032, (2016), 5 p.

Bjornsson, S., Arnorsson, S. and Tomasson, J.: Economic Evaluation of Reykjanes Thermal Brine Area, Iceland. *American Association of Petroleum Geologists Bulletin*, **56**, (1972), 2380-2391.

Bodvarsson, G. and Walker, G.P.L.: Crustal Drift in Iceland. *The Geophysical Journal of the Royal Astronomical Society*, **8**, (1964), 285-300. https://doi.org/10.1111/j.1365-246X.1964.tb06295.x

Clifton, A.E. and Kattenhorn, S.A.: Structural Architecture of a Highly Oblique Divergent Plate Boundary Segment. *Tectonophysics*, **419**, (2006) 27-40. https://doi.org/10.1016/j.tecto.2006.03.016

Dauteuil, P. and Brun, J.P.: Deformation Partitioning in a Slow-Spreading Ridge Undergoing Oblique Extension (Mohns Ridge-Norwegian Sea). *Tectonics*, **15**, (1996), 870-884. https://doi.org/10.1029/95TC03682

DeMets, C., Gordon, R.G., Argus, D.F. and Stein, S.: Effect of Recent Revisions to the Geomagnetic Reversal Time Scale on Estimates of Current Plate Motions. *Geophysical Research Letters*, **21**, (1994), 2191-2194.

Einarsson, P.: Plate Boundaries, Rifts and Transforms in Iceland. *Jökull*, **58**, (2008), 35-58.

Eiríksson, J.: Lithostratigraphy of the Upper Tjörnes Sequence, North Iceland: The Breidavík Group. *Acta Naturalia Islandica*, **29**, (1981), 37 p.

Franzson, H.: The Reykjanes High-Temperature Geothermal System. Geological and Geothermal Model. Iceland GeoSurvey Report, ISOR-2004/012, (2004), 60 p. (In Icelandic)

Friðleifsson, G.Ó., Elders, W.A., Zierenberg, R.A., Fowler, A.P.G., Weisenberger, T.B., Mesfin, K.G., Sigurðsson, Ó., Níelsson, S., Einarsson, G., Óskarsson, F., Guðnason, E.Á., Tulinius, H., Hokstad, K., Benoit, G., Nono, F., Loggia, D., Parat, F., Cichy, S.B., Escobedo, D., Mainprice, D., The Iceland Deep Drilling Project at Reykjanes: Drilling into the root zone of a black smoker analog. *Journal of Volcanology and Geothermal Research*, (2018), in press, https://doi.org/10.1016/j.jvolgeores.2018.08.013

Gislason, G., Johnsen, G.V., Armannsson, H., Torfason, H. and Arnason, K.: Theistareykir: Surface Exploration in the High-Temperature Field. National Energy Authority Report, OS-84089/JHD-16, (1984), 134 p, 3 maps.

Guðnason, E.A. and Ágústsson, K. Earthquake Swarm on Reykjanes in October 2013. Iceland GeoSurvey Report, ISOR-2014/017, (2014), 25 p.

Guðnason, E.A., Ágústsson, K., Gunnarsson, K. and Flóvenz, O.G.: Seismic activity on Reykjanes December 2014-December 2015. Iceland GeoSurvey Report, ISOR-2015/068, (2015), 31 p.

Harðarson, B.S., Fitton, J.G., Ellam, R.M. and Pringle, M.S.: Rift Relocation - A Geochemical and Geochronological Investigation of a Palaeo-Rift in Northwest Iceland. *Earth and Planetary Science Letters*, **153**, (1997), 181-196.https://doi.org/10.1016/S0012-821X(97)00145-3

Hjaltadóttir, S. and Vogfjörð, K.: Fracture Mapping at Theistareykir and Bjarnarflag with High Resolution Location of Microearthquakes. Landsvirkjun Report LV-2011-116, (2011), 44 p. (in Icelandic).

Homberg, C., Bergerat, F., Angelier, J. and Garcia, S.: Fault Interaction and Stresses along Broad Oceanic Transform Zone: Tjornes Fracture Zone, North Iceland. *Tectonics*, **29**, (2010), TC1002. https://doi.org/10.1029/2008TC002415

Hoskuldsson, A., Kjartansson, E. and Hey, R.: Seabed Research on the Reykjanes Ridge. *Proceedings* of the 2004 Spring Conference, Icelandic Geological Society (JFI), (2004), 10-12.

Jakobsdóttir, S.S.: Seismicity in Iceland: 1994-2007. *Jökull*, **58**, (2008), 75-100.

Karlsdóttir, R., Vilhjálmsson, A.M., Arnason, K. and Beyene, A.T.: Þeistareykir Geothermal Area, Northern Iceland. 3D Inversion of MT Data. Iceland GeoSurvey Report, ISOR-2012/046, (2012), 173 p.

Karlsdóttir, R., Vilhjálmsson, A.M. and Guðnason, E.Á.: Three dimensional inversion of magnetotelluric (MT) resistivity data from Reykjanes high temperature area. *Journal of Volcanology and Geothermal Research*, (2018), in press. https://doi.org/10.1016/j.jvolgeores.2018.11.019..

Khodayar, M., and Einarsson, P.: Strike-slip faulting, normal faulting and lateral dyke injections along a single fault: Field example of the Gljúfurá Fault near a Tertiary oblique rift/transform zone, Borgarfjörður, W-Iceland. *Journal of Geophysical Research*, **107**, **B5**, (2002),10.1029/2001JB000150, (ETG 5, p. 1-18).

Khodayar, M., Björnsson, S., Axelsson, G., Nielsson, S., and Franzson, H.: Preliminary Structural Analysis of Reykjanes for Re-injection. Prepared for HS Orka /Alterra Power. Report Iceland GeoSurvey, ÍSOR-2014/039, (2014), 96 p., 1 Map (Confidential report).

Khodayar, M., and Björnsson, S.: Structures and Styles of Deformation in Rift, Ridge, Transform Zone, Oblique Rift and a Microplate Offshore/Onshore North Iceland. *International Journal of Geosciences*, **9**, (2018), 461-511. https://doi.org/10.4236/ijg.2018.98029

Khodayar, M.: Shift of a rift by a transform zone: a case from the Northern Rift Zone and Tjörnes Fracture Zone of Iceland. *Petroleum Geoscience*, **24**, (2018), 414-424. First published online April 7, 2018. https://doi.org/10.1144/petgeo2016-132

Khodayar, M., Bjornsson, S., Guðnason, E.A., Nielsson, S.,Axelsson, G. and Hickson, C.: Tectonic Control of the Reykjanes Geothermal Field in the Oblique Rift of SW Iceland:From Regional to Reservoir Scales. *Open Journal of Geology*, **8**, (2018a), 333-382. https://doi.org/10.4236/ojg.2018.83021

Khodayar, M., Bjornsson, S., Kristinsson, S.G., Karlsdottir, R., Olafsson, M. and Vikingsson, S.: Tectonic Control of the Theistareykir Geothermal Field by Rift and Transform Zones in North Iceland: A Multidisciplinary Approach. *Open Journal of Geology*, **8**, (2018b), 543-584. https://doi.org/10.4236/ojg.2018.86033

Klein F.W., Einarsson, P. and Wyss, M.: The Reykjanes Peninsula, Iceland, Earthquake Swarm of September 1972 and Its Tectonic Significance. *Journal of Geophysical Research*, **82**, (1977), 856-888. https://doi.org/10.1029/JB082i005p00865

Kristinsson, S.G., Oskarsson, F., Oladottir, A.A. and Olafsson, M.: The High Temperature Geothermal Areas at Þeistareykir, Krafla and Namafjall. Monitoring of Surface Geothermal Activity and Groundwater in the Year 2015 (in Icelandic). Iceland GeoSurvey Report ISOR-2015/059, LV-2015-125, (2015), 175 p.

Kristjánsson, L.: Paleomagnetic Research on Icelandic Lava Flows. *Jökull*, **58**, (2008), 101-116.

McDougall, I., Saemundsson, K., Johannesson, H., Watkins, N.D. and Kristjansson, L.: Extension of the Geomagnetic Time Scale to 6.5 m.y.: K-Ar Dating, Geological and Paleomagnetic Study of a 3,500 m Lava Succession in Western Iceland. *Bulletin of Geological Society of America*, **88**, (1977), 1-15. https://doi.org/10.1130/0016-7606(1977)88<1:EOTGPT>2.0.CO;2

Palgan, D., Devey, C.W. and Yeo, I.A.: Volcanism and Hydrothermalism on a Hotspot-Influenced Ridge: Comparing Reykjanes Peninsula and Reykjanes Ridge, Iceland. *Journal of Volcanology and Geothermal Research*, **348**, (2017), 62-81. https://doi.org/10.1016/j.jvolgeores.2017.10.017

Rögnvaldsson, S., Guðmundsson, A. and Slunga, R.: Seismotectonic Analysis of the Tjörnes Fracture Zone, an Active Transform Fault in North Iceland. *Journal of Geophysical Research*, **103**, (1998), 117-130. https://doi.org/10.1029/98JB02789

Sigmundsson, F., Hooper, A., Hreinsdottir, S., Vogfjord, K.S., Ofeigsson, B.G., Heimisson, E.R., Dumont, S., Parks, M., Spaans, K., Gudmundsson, G.B., Drouin, V., Arnadottir, T., Jonsdottir, K., Gudmundsson, M.T., Hognadottir, T., Fridriksdottir, H.M., Hensch, M., Einarsson, P., Magnusson, E., Samsonov, S., Brandsdottir, B., White, R.S., Agustsdottir, T., Greenfield, T., Green, R.G., Hjartardottir, A.R., Pedersen, R., Bennett, R.A., Geirsson, H., La Femina, P.C., Bjornsson, H., Palsson, F., Sturkell, E., Bean, C.J., Mollhoff, M., Braiden, A.K. and Eibl, E.P.S.: Segmented Lateral Dyke Growth in a Rifting Event at Bardarbunga Volcanic System, Iceland. *Nature*, **517**, (2015), 191-195. https://doi.org/10.1038/nature14111

Símonarson, L. and Eiríksson, J.: Tjörnes - Pliocene and Pleistocene Sediments and Fauna. *Jökull*, **58**, (2008), 331-342.

Stefánsson, R., Guðmundsson, G.B. and Halldórsson, P. Tjörnes Fracture Zone. New and Old Seismic Evidences for the Link between the North Iceland Rift Zone and the Mid-Atlantic Ridge. *Tectonophysics*, **447**, (2008), 117-126. https://doi.org/10.1016/j.tecto.2006.09.019

Steinthorsson, S., Oskarsson, N., Arnorsson, S. and Gunnlaugsson, E.: Metosomatism in Iceland: Hydrothermal Alteration and Remelting of Oceanic Crust. *NATO ASI Chemical Transport to Metasomatic Processes*, Attica, (1986), 355-387.

Sæmundsson, K.: Fissure Swarms and central Volcanoes of the Neovolcanic Zones of Iceland. In: Crustal Evolution in Northwestern Britain and Adjacent Regions. *Geological Journal*, Special Issue, **10**, (1978), 415-432.

Sæmundsson, K., Hjartarson, Á., Kaldal, I., Sigurgeirsson, M.Á., Kristinsson, S.G. and Víkingsson, S.: Geological Map of Northern Volcanic Zone, Iceland. Northern Part. 1:100.000, (2012), Reykjavík. Iceland GeoSurvey and Landsvirkjun.

Thoroddsen, Th.: Die Geschichte der Isländischen Vulkane. *Det Kongelige Danske Vidernskabernes Selskab*, Höst og Sön, Copenhagen, (1925).

Trippanera, D., Acocella, V., Ruch, J. and Abebe, B.: Fault and Graben Growth along Active Magmatic Divergent Plate Boundaries in Iceland and Ethiopia. *Tectonics*, **34**, (2015), 2318-2348. https://doi.org/10.1002/2015TC003991

Walker G.P.L.: Zeolite Zones and Dike Distribution in Relation to the Structure of the Basalts of Eastern Iceland. *Journal of Geology*, **68**, (1960), 515-528. https://doi.org/10.1086/626685